Chemical Science

ROYAL SOCIETY OF CHEMISTRY

EDGE ARTICLE

View Article Online
View Journal | View Issue

Check for updates

Cite this: *Chem. Sci.*, 2023, **14**, 2935

All publication charges for this article have been paid for by the Royal Society of Chemistry

Received 6th December 2022
Accepted 14th February 2023

DOI: 10.1039/d2sc06704h

rsc.li/chemical-science

# Acid-induced nitrite reduction of nonheme iron(II)-nitrite: mimicking biological Fe–NiR reactions†

Kulbir, [a] Sandip Das, [a] Tarali Devi,[c] Somnath Ghosh, [a] Subash Chandra Sahoo [b] and Pankaj Kumar *[a]

Nitrite reductase (NiR) catalyzes nitrite ($NO_2^-$) to nitric oxide (NO) transformation in the presence of an acid ($H^+$ ions/pH) and serves as a critical step in NO biosynthesis. In addition to the NiR enzyme, NO synthases (NOSs) participate in NO production. The chemistry involved in the catalytic reduction of $NO_2^-$, in the presence of $H^+$, generates NO with a $H_2O$ molecule utilizing two $H^+$ + one electron from cytochromes and is believed to be affected by the pH. Here, to understand the effect of $H^+$ ions on $NO_2^-$ reduction, we report the acid-induced $NO_2^-$ reduction chemistry of a nonheme $Fe^{II}$-nitrito complex, $[(12TMC)Fe^{II}(NO_2^-)]^+$ ($Fe^{II}$–$NO_2^-$, **2**), with variable amounts of $H^+$. $Fe^{II}$–$NO_2^-$ upon reaction with one-equiv. of acid ($H^+$) generates $[(12TMC)Fe(NO)]^{2+}$, $\{FeNO\}^7$ (**3**) with $H_2O_2$ rather than $H_2O$. However, the amount of $H_2O_2$ decreases with increasing equivalents of $H^+$ and entirely disappears when $H^+$ reaches ≅ two-equiv. and shows $H_2O$ formation. Furthermore, we have spectroscopically characterized and followed the formation of $H_2O_2$ ($H^+$ = one-equiv.) and $H_2O$ ($H^+$ ≅ two-equiv.) and explained why bio-driven NiR reactions end with NO and $H_2O$. Mechanistic investigations, using $^{15}N$-labeled-$^{15}NO_2^-$ and $^2H$-labeled-$CF_3SO_3D$ ($D^+$ source), revealed that the N atom in the $\{Fe^{14/15}NO\}^7$ is derived from the $NO_2^-$ ligand and the H atom in $H_2O$ or $H_2O_2$ is derived from the $H^+$ source, respectively.

Nitric oxide (NO), a critical biological component, participates in numerous bio-physiological processes such as neurotransmission, vascular regulation, inhibiting platelet aggregation, and immune response to multiple infections at nanomolar concentration.[1] Also, NO is known to be involved in plant growth and development.[2] NO meagerness may cause pathogenic effects such as atherosclerosis, diabetic hypertension, *etc.*[3] However, at micromolar concentrations, NO is highly toxic and utilized for immune defense against harmful pathogens,[4] in addition to its oxidized species, *i.e.*, peroxynitrite ($ONOO^-$)[5] or/nitrogen dioxide ($^{\bullet}NO_2$).[6] In contrast to the immune response towards pathogens, oxidized NO species also show various toxicological actions in biological systems.[5b,7]

Hence, sensible production of NO is required to maintain physiological homeostasis and is usually achieved by two metalloenzymes, *i.e.*, NO synthases (NOSs)[8] and/or nitrite reductases (NiRs).[8a,9] NOS enzymes are heme-proteins that generate NO by catalyzing the conversion of L-arginine to L-citrulline under aerobic conditions.[8b,c] However, under ischemia and hypoxic conditions, the suppression of NOS activity results in the decrease of NO generation. Under such conditions, $NO_2^-$ works as an active NO source in biological systems, generating NO in acid-induced $NO_2^-$ reduction reactions.[10] Sometimes, under abnormal conditions, biochemical dysfunction may cause NO overproduction by NiRs or NOSs. Under such conditions, NO dioxygenase (NOD) enzymes available *in vivo* convert excess NO to biologically benign nitrate ($NO_3^-$).[11] $NO_3^-$, the product of the NOD reaction, serves as a critical component of $NO_2^-$ generation and a precursor to the biological NO cycle.[12] In humans, commensal bacteria in the oral cavity play a vital role in converting $NO_3^-$ to $NO_2^-$.[12a] Bacteria reduce $NO_3^-$ to $NO_2^-$ *via* an OAT reaction mediated by molybdenum-based NR enzymes.[13] The interconversion of $NO_3^-$ to/$NO_2^-$/to NO (or *vice versa*) is the critical step of the denitrification process.[14] *In vivo* studies have proven that $NO_2^-$ is a fundamental source of NO in mammalian or bacterial systems, an intermediate species of the biological nitrogen cycle ($NO_3^-$ → $NO_2^-$ → NO → $N_2O$ → $N_2$).[14] At the bio-physiological level, $NO_2^-$ gets reduced to NO, primarily by globins[15] or by acid-catalyzed $NO_2^-$ reduction in the stomach[16,17] or by Fe/Cu-NiR enzymes/cytochrome c oxidase (CcO)/xanthine oxidase,[18] which reduces $NO_2^-$ to NO in the presence of two-equiv. of $H^+$ ions, *i.e.*,[8a,9,15]

$$NO_2^- + e^- + 2H^+ \rightarrow NO + H_2O \quad (1)$$

[a]*Department of Chemistry, Indian Institute of Science Education and Research (IISER), Tirupati 517507, India. E-mail: pankajatiisert@gmail.com; pankaj@iisertirupati.ac.in*

[b]*Department of Chemistry, Punjab University, Chandigarh, Punjab, India*

[c]*Humboldt-Universität zu Berlin, Institut für Chemie, Brook-Taylor-Straße 2, D-12489 Berlin, Germany*

† Electronic supplementary information (ESI) available. CCDC 2181978 and 2181979. For ESI and crystallographic data in CIF or other electronic format see DOI: https://doi.org/10.1039/d2sc06704h

Open Access Article. Published on 23 February 2023. Downloaded on 9/21/2023 12:58:10 AM. This article is licensed under a Creative Commons Attribution-NonCommercial 3.0 Unported Licence.

Open Access Article. Published on 23 February 2023. Downloaded on 9/21/2023 12:58:10 AM. This article is licensed under a Creative Commons Attribution-NonCommercial 3.0 Unported Licence.

However, few functional mimicking models were developed and investigated *in vivo*/*in vitro* to explore the mechanistic insight of microbial NiR enzymatic chemistry. Brooks and coworkers proposed the NiR activity of mammalian hemoglobin (Hb) protein under anaerobic conditions, which converts $NO_2^-$ to NO with the formation of metHb.[19] E. T. Papish *et al.* explored the Cu-NiR chemistry and showed NO production with $H_2O$ as a side product *via* a $Cu^I$–$NO^+$ ↔ $Cu^{II}$–NO intermediate in the reaction of Cu–$NO_2^-$ with two-equiv. of $H^+$.[20] A heme-Fe/Cu assembly model has been developed to mimic the cytochrome c oxidase, illustrating the reversible conversion of $NO_2^-$ to NO.[21] For the first time, Murphy and coworkers explored the explained Cu–$NO_2^-$ reduction reaction to release NO *via* the {CuNO} intermediate and characterized it structurally.[9b,22] Patra and coworkers have mimicked $NO_2^-$ reduction reactivity using $Cu^{II}$–$NO_2^-$ with two-equiv. of $H^+$ and one $e^-$, leading to NO and $H_2O$ molecule formation.[23] Lehnert and coworkers have explored electrocatalytic reduction using $Cu^{II}$–$NO_2^-$ producing NO in aqueous media[24] and compiled the electronic structure and reactivity of the biologically relevant coordination chemistry of iron and NO.[15] In addition to acid-encouraged $NO_2^-$ reduction to NO in different model systems. Various models have been explored for the reduction of metal-bound $NO_2^-$ to NO *via* (i) oxygen atom transfer (OAT) caused by ($R_2S$)[25]/thiol (RSH)}[18a,26]/triphenylphosphine ($PPh_3$)[27]/vanadium chloride ($VCl_3$)[28] and (ii) photo-induced reactions[29] of metal–bound nitrite (M–$NO_2^-$).

In addition to the developments on biomimetic synthetic modeling of M–NOs/or active sites associated with NiR and/or NOS.[11d,30] Recently, Lehnert and coworkers have established the synthetic strategy for Fe–NOs,[31] and Nam and coworkers have explored the photo-induced NiR reactivity of Fe–$NO_2^-$ to generate Fe–NOs and also stabilize Co–NOs.[32] Ford and coworkers continuously discover the NiR chemistry of various heme systems.[33] Although NiR is the key source of NO in the biological system, such reactions are not investigated extensively to characterize the intermediates and transition states of $NO_2^-$ reduction reactions. Hence, several research groups are working to understand the proper $NO_2^-$ reduction reaction mechanism. There are only very few reports on acid-induced $NO_2^-$ reduction reactions to mimic NiR enzymatic reactions and understand the mechanistic aspects.[9b,29,34] In this investigation, we intend to characterize different intermediates of $H^+$-induced $NO_2^-$ reduction in $Fe^{II}$–$NO_2^-$ and its reaction products and then explore its mechanistic aspects. This report will focus on how different amounts of acid ($H^+$ ion) affect the reaction mechanism and regulate the side products in addition to NO.

Herein, we report the $NO_2^-$ reduction chemistry of a nonheme FeII–$NO_2^-$ complex, [(12TMC)$Fe^{II}$($NO_2^-$)]$^+$ (**2**), bearing the 1,4,7,10-tetramethyl-1,4,7,10-tetraazacyclododecane (12TMC) ligand (Scheme 1, reaction I). Complex **2** reacts with one-equiv. of triflic acid (HSO3CF3, $H^+$ source) and generates the corresponding nonheme Fe–nitrosyl complex, [(12TMC)Fe(NO)]$^{2+}$({FeNO}, **3**), and $H_2O_2$ (Scheme 1, reactions II & III) in CH3CN at 233 K. However, upon reaction with a base ($OH^-$), **2** does not form **3**. Mechanistic investigations using $^{15}$N-labeled-$^{15}NO_2^-$ demonstrated explicitly that the N atom in the NO moiety of **3** is derived from the $NO_2^-$ anion and $H_2O_2$ by the protonation of the O atom of the $NO_2^-$ moiety. Conversely, an increased $H^+$ concentration showed a significant fall in $H_2O_2$, which disappeared completely when the $H^+$ ion quantity was ≅ two-equiv. with the simultaneous formation of a substantial amount of $H_2O$ (Scheme 1, reaction IV). To the extent of our knowledge, the present work reports the very first comparative study for the reaction of an $Fe^{II}$–$NO_2^-$ complex with varying $H^+$ concentrations and the evidence showing the formation of $H_2O_2$ (one-equiv. of $H^+$) and $H_2O$ (≅ two-equiv. of $H^+$), illustrating a new approach for NiR enzyme activity (Scheme 1).

## Results and discussion

### Preparation of the $Fe^{II}$-nitrito complex, [(12-TMC)$Fe^{II}$($NO_2^-$)]$^+$ (2)

The initial FeII–$NO_2^-$ complex, [(12TMC)$Fe^{II}$($NO_2^-$)]$^+$ (**2**), was prepared by the addition of one equivalent of $NaNO_2$ in the presence of a 15-crown-5 to $Fe^{II}$-complex, [(12TMC)$Fe^{II}$($NCCH_3$)]$^{2+}$ (**1**), in CH3CN at 298 K (Scheme 1 & reaction I; also see the ESI and Experimental section (ES)). Complex **2** was further characterized by various spectroscopic measurements, including the determination of the single-crystal X-ray structure. A UV-vis absorption band ($\lambda_{max}$ = 325 nm and $\varepsilon$ = 356 $M^{-1}$ $cm^{-1}$) was formed upon adding an equivalent amount of $NaNO_2$ to the $CH_3CN$ solution of **1**, which corresponds to **2** (Fig. 1a). A characteristic peak for metal-bound $NO_2^-$ stretching at 1270 $cm^{-1}$ was observed in the FT-IR spectrum of **2**, which shifted to 1247 $cm^{-1}$ when **2** was prepared using $^{15}$N-labeled-nitrite ($^{15}N^{16}O_2^-$) (inset: Fig. 1a andS1; ESI†).[35] The electrospray ionization mass spectrum (ESI-MS) recorded for **2** showed a prominent ion peak at *m*/*z* 330.1, which shifted to m/*z* 331.1 when prepared with $^{15}$N-labeled $Na^{15}N^{16}O_2$, and their mass and isotope distribution pattern corresponds to [(12TMC)Fe($NO_2^-$)]$^+$ (calc. *m*/*z* 330.1) and [(12TMC)Fe($^{15}NO_2^-$)]$^+$ (calc. *m*/*z* 331.1), respectively (Fig. 1b and S2; ESI†). The $^1$H-NMR spectrum of **2** showed fairly clean paramagnetic proton signals for the protons of the 12TMC ligand (Fig. S3a†), suggesting a magnetically active Fe center. The spin-state of the Fe center in **2** was determined by calculating the magnetic moment of the $Fe^{II}$ center by Evans' method and found to be 5.19 BM, suggesting a high spin $Fe^{II}$ ion (*S* = 2) in complex **2** (ESI,† ES, Fig. S3b). The electrochemical measurement of **2** showed

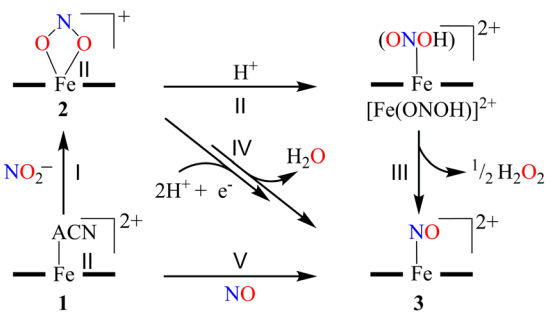


Scheme 1


© 2023 The Author(s). Published by the Royal Society of Chemistry

Open Access Article. Published on 23 February 2023. Downloaded on 9/21/2023 12:58:10 AM.
This article is licensed under a Creative Commons Attribution-NonCommercial 3.0 Unported Licence.

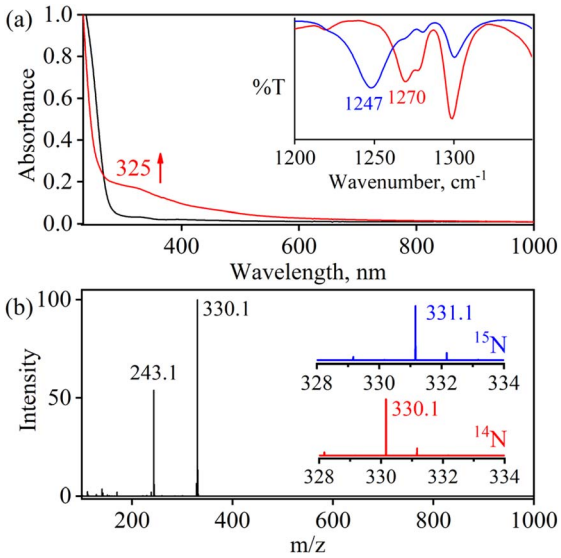


Fig. 1 (a) UV-visible spectra of **1** (0.50 mM, black line) and **2** (0.50 mM, red line) in $CH_3CN$ under Ar at 298 K. Inset: IR spectra of **2**-$^{14}NO_2^-$ (red line) and **2**-$^{15}NO_2^-$ (blue line) in KBr. (b) ESI-MS spectra of **2**. The peak at 330.1 is assigned to $[(12TMC)Fe^{II}(NO_2^-)]^+$ (calcd *m/z* 330.1). Inset: isotopic distribution pattern for **2**-$^{14}NO_2^-$ (red line) and **2**-$^{15}NO_2^-$ (blue line).

a reversible cyclic voltammogram (redox potential + 0.56 V *vs.* $Ag/AgNO_3^-$) (ESI, Fig. S4a†). In addition to the above spectral measurements, the structural details of **2** were obtained by its single-crystal X-ray structure determination (Fig. 2). The $Fe^{II}$ center of **2** was found to have O, O′-chelated bi-dentate $NO_2^-$ anions in a distorted octahedral geometry (ESI,† ES, Fig. S5 and Tables 1 & 2).

### The nitrite reduction reaction of the $Fe^{II}$–$NO_2^-$ complex (2)

To further investigate the $NO_2^-$ reduction chemistry of FeII–$NO_2^-$ (**2**), we explored its reaction with different equivalents of acid ($H^+$ ions). When **2** was reacted with H+, we observed a visible color change from yellow to green and a new absorption band ($\lambda_{max} = 350$ nm and $\varepsilon = 1450\ M^{-1}\ cm^{-1}$), characteristic of a new species (**3**), formed over ~2 minutes in CH3CN under Ar at 233 K (Fig. 3a; ESI,† ES, and Fig. S6).[8a,9] Complex **2** was found to be very stable in $CH_3CN$ and at 298 K as it did not show any spectral variations in the absence of $H^+$ (ESI,† Fig. S7a). Complex **2** was also found inert towards $OH^-$ as it does not indicate any change in UV-vis spectra when treated with tetrabutylammonium hydroxide (ESI, Fig. S7b†), suggesting that Fe–$NO_2^-$ reacts only with $H^+$. The amount of $H^+$ required to reduce the $NO_2^-$ moiety was determined by spectral titration, which confirmed the ratio-metric equivalent of **2** with $H^+$ as 1 : 1 (ESI,† Fig. S8). The compound **3**, obtained in the reaction of **2** with H+ was determined to be an Fe–nitrosyl complex, $\{FeNO\}^7$, based on various spectroscopic characterization techniques (*vide infra*). The other product of the $NO_2^-$ reduction using one-equiv. of $H^+$ was determined to be $H_2O_2$, in contrast to previous reports on biological NiR and $NO_2^-$ reduction chemistry, *via* a proposed thermally unstable ONOH intermediate as reported in the literature (Scheme 1, reactions II & III).[36] However, when reacted with more than one-equiv. of $H^+$ (≅ two) **2** generated **3**, but the amount of $H_2O_2$ decreased gradually with

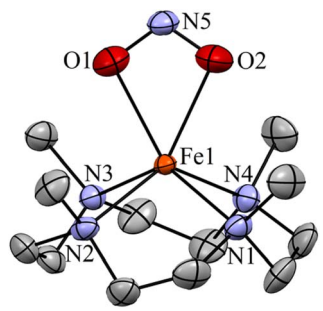


Fig. 2 Displacement ellipsoid plot (15% probability) of **2** at 100 K. Disorder C atoms of TMC, anions and H atoms have been removed for clarity.

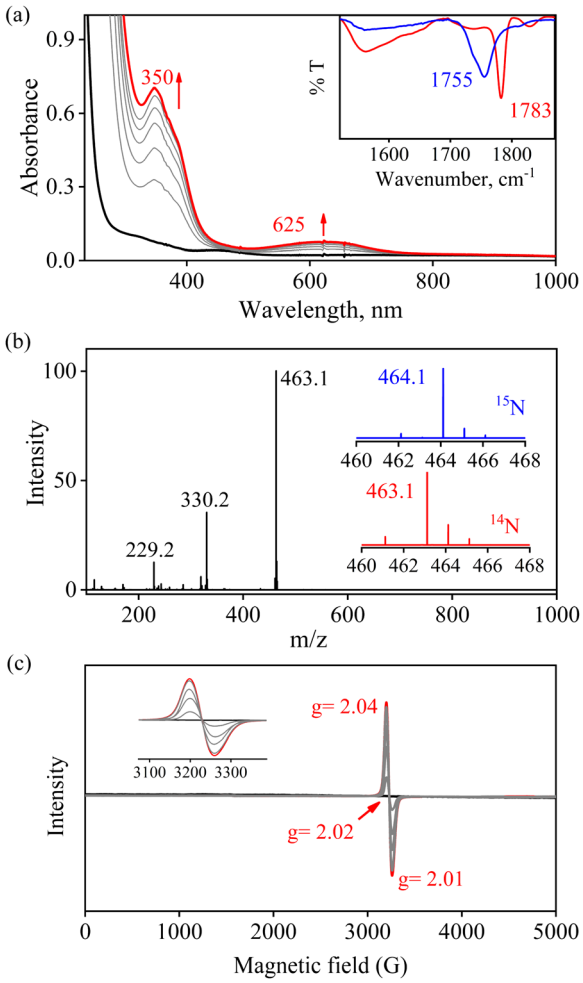


Fig. 3 (a) UV-visible spectral changes of **2** (0.50 mM, black line) upon addition of $H^+$ (one-equiv.) in $CH_3CN$ at 233 K. Black line (**2**) changed to a red line (**3**) upon addition of $H^+$. Inset: IR spectra **3**-$^{14}NO$ (red line) and **3**-$^{15}NO$ (blue line) in KBr. (b) ESI-MS spectra of **3**. The peak at 463.1 is assigned to [(12TMC)FeII(NO)(OTf)]+ (calcd *m/z* 463.1). Inset: isotopic distribution pattern for **3**-14NO (red line) and **3**-15NO (blue line). (c) Time-dependent EPR spectra of the generation of **3** (red line) in the reaction of **2** and $H^+$ (one-equiv.) in $CH_3CN$ at 77 K.

Open Access Article. Published on 23 February 2023. Downloaded on 9/21/2023 12:58:10 AM. This article is licensed under a Creative Commons Attribution-NonCommercial 3.0 Unported Licence.

increasing $H^+$. This suggests the decomposition of $H_2O_2$ or utterly new chemistry in the presence of more than one-equiv. of $H^+$; the new product was confirmed to be $H_2O$ by using various spectral measurements (Scheme 1, reaction IV). To the best of our knowledge, this work reports the first-ever study where the side products of $NO_2^-$ reduction are regulated by different amounts of $H^+$, which opens a new pathway of acid-induced $NO_2^-$ reduction chemistry to the scientific community.

We have performed various spectral measurements to track the products of $H^+$ (or $D^+$)-induced reduction of Fe-bound $^{14/15}NO_2^-$ in **2**. The FT-IR spectrum of **3** showed a characteristic peak for Fe-bound nitrosyl stretching at 1783 $cm^{-1}$ ($\{Fe^{14}NO\}^7$), which shifted to 1755 $cm^{-1}$ ($\{Fe^{15}NO\}^7$) when **3** was prepared by the reaction of $^{15}N$-labeled-nitrite (**2**-$^{15}NO_2^-$) with one-equiv. of $H^+$ (inset, Fig. 3a and S9; ESI†). This shifting in NO stretching frequency ($\Delta = 28$ $cm^{-1}$) indicates that the N atom in NO moiety is derived from the $^{14/15}NO_2^-$ ligand of **2**. Similarly, the ESI-MS spectrum of **3** showed a prominent peak at *m*/*z* 463.1, [(12TMC)Fe(NO)(OTf)]$^+$ (calc. *m*/*z* 463.1), which shifted to 464.1, [(12TMC)Fe($^{15}$NO)(OTf)]$^+$ (calc. *m*/*z* 464.1), when $Fe^{II}$–$^{15}NO_2^-$ was reacted with $H^+$ (Fig. 3b and S10; ESI†), specifying clearly that NO in **3** is derived from the $NO_2^-$ moiety. The $^1$H-NMR spectrum of **3** showed shifting in the $^1$H-signals of the 12TMC ligand framework suggesting a paramagnetic system (ESI, Fig. S11a†).[32a,b] We determined the spin-state of the Fe centre in **3** by calculating its magnetic moment using Evans' method and found it to be 2.3 BM, suggesting a low-spin Fe center in **3** (S = 1/2) for the complex **3** (ESI, ES, and Fig. S11b†).[37] Additionally, time-dependent EPR measurements were followed for the generation of **3** in the reaction mixture of **2** + $H^+$. EPR measurements (77 K), performed at different time intervals, showed the formation of a new species ($g = 2.04$) (Fig. 3c), which is characteristic of the EPR signal of isolated species $\{FeNO\}^7$ (Scheme 1, reaction V), confirming the formation of low-spin **3** in the above reaction (ESI, Fig. S11c†). The electrochemical measurement of **3** showed a reversible cyclic voltammogram (redox potential + 0.36 V *vs.* Ag/$AgNO_3^-$) (ESI, Fig. S4b†). Additionally, we have determined the binding constants $K_b(Fe^{II}–NO_2^-)$ and $K_b\{(Fe(NO)\}^7$ using the Benesi–Hildebrand equation[28,38] for the generation of **2** and **3** in the reaction of $[(12TMC)Fe^{II}(CH_3CN)]^{2+}$ with $NO_2^-$ and NO. The values were $K_b(Fe^{II}–NO_2^-) = 4.7 \times 10^2$ $M^{-1}$ & $K_b\{(FeNO\} = 8.4 \times 10^2$ $M^{-1}$ (ESI,† ES, and Fig. S12), which also supports the forward reaction. In addition, the yield for the formation of **3** was calculated by comparing the UV-vis absorption spectra of **3** formed in the reaction of **2** with one-equiv. of $H^+$ with the authentic Fe–nitrosyl complex ($\{FeNO\}^7$), prepared in a separate reaction of $[(12TMC)Fe^{II}(CH_3CN)]^{2+}$ + NO, and was found to be 95%. However, the yield decreased to 85% when the reaction was carried out using two-equiv of $H^+$ (ESI, ES, and Fig. S13†). Furthermore, the structural details of **3**, obtained in the reaction of **2** and $H^+$, were obtained by its single-crystal X-ray structure determination (ESI, ES & Fig. 4). The NO moiety showed the coordination *via* the N atom to the Fe center of **3** with the a angle of 168° (ESI, ES Fig. S14;† & Tables T1 and T2). This arrangement suggests a neutral $^{\bullet}$NO moiety with an $Fe^{II}$ center[37,39] (further supported by BVS calculation from the crystal parameters of **3**, ESI,† ES) and can be formulated as

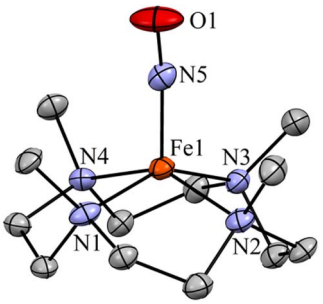


Fig. 4 Displacement ellipsoid plot (50% probability) of **3** at 100 K. Disordered C atoms of TMC, anions and H atoms have been removed for clarity.

[(12TMC)$Fe^{II}$(NO)]$^{2+}$; however, in this manuscript, we used Enemark–Feltham notation for **3** ($\{FeNO\}^7$).

## Mechanistic investigation of $NO_2^-$ reduction

*In vivo* and *in vitro* biomimetic studies on acid-induced $NO_2^-$ reduction reactions produce NO with $H_2O$ (as explained in the biological NiR chemistry)[34a,40] or in some cases $^{\bullet}$OH ($H_2O_2$)[36] or a metal hydroxide[41] and should be accomplished *via* the proposed ONOH intermediate, as reported by Murphy *et al.*,[9b] and Rose *et al.*[40g] for the biological Cu-NiR chemistry. Similarly, Fujii and coworkers also proposed a Cu(ONOH) intermediate in the acid-induced biomimetic $NO_2^-$ reduction on the $Cu^I$ center.[40h] Meanwhile, Shigeta *et al.*[40i] & Chen and coworkers[40j] theoretically established the presence of a Cu(ONOH) intermediate in acid-induced $NO_2^-$ reduction. The present work elucidated how varying equivalents of $H^+$ ions determine the side products of $Fe^{II}$-bound $NO_2^-$ reduction chemistry in addition to NO and should be accomplished by a similar proposed ONOH intermediate. In this regard, we proposed the reaction sequences, where the preliminary step of the $NO_2^-$ reduction reaction consists of an electrophilic addition of $H^+$ to the $NO_2^-$ anion of **2** and generating the suggested $[Fe–ONOH]^{2+}$ intermediate species (Scheme 2, reaction I), as proposed previously.[36,41] The presumed $[Fe–(ONOH)]^{2+}$ intermediate is believed to produce $\{FeNO\}^7$ *via* the homolytic cleavage of the ON–OH moiety, as reported in $NO_2^-$ reduction on

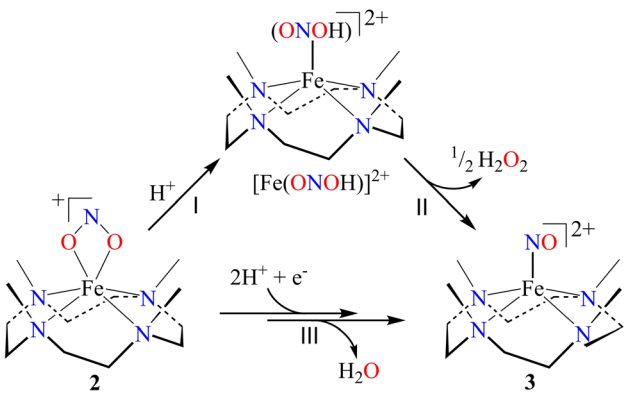


Scheme 2


© 2023 The Author(s). Published by the Royal Society of Chemistry

Open Access Article. Published on 23 February 2023. Downloaded on 9/21/2023 12:58:10 AM.
This article is licensed under a Creative Commons Attribution-NonCommercial 3.0 Unported Licence.

the $Fe^{II}$ center and Cu-NiR,[36,41] and $^{\bullet}OH$ ($^1/_2$ $H_2O_2$)[42] (Scheme 2, reaction II). In contrast, $NO_2^-$ reduction in the presence of ≈ two-equiv. or more $H^+$ produced **3** with $H_2O$ as a side product in a multiple-step reaction (Scheme 2, reaction III). This reaction is believed to occur *via* the reduction of the $NO_2^-$ anion of **2** in the presence of two $H^+$, as reported in biological NiR[9b,40g] and biomimetic $NO_2^-$ reduction[40h–j,43] reactions. The $H_2O$ molecule may be generated either by (a) step-wise protonation of $NO_2^-$ species of **2** as observed in biology,[40a,b] (b) acidic decomposition of $H_2O_2$,[44] or (c) by auto-decomposition of $H_2O_2$.[45]

To validate our proposed $H^+$-induced $NO_2^-$ reduction chemistry mechanism, we have reacted **2** with different equivalents of $H^+$ and characterized all the products formed in the reaction mixture. In both the acid-induced reactions, we observed the formation of **3**. However, the side product of $NO_2^-$ reduction changed to $H_2O$ instead of $H_2O_2$ when the $H^+$ amount was ≥ two-equiv. (ESI,† ES). $H_2O_2$/& $H_2O$ formed in the $NO_2^-$ reduction reaction was followed/characterized and quantified using $^1$H-NMR spectroscopic measurements. A characteristic signal for $H_2O_2$ (8.66 ppm, ESI,† Fig. S15a)[46] was observed in the $^1$H-NMR spectrum of **2** with one-equiv. of $H^+$ in $CD_3CN$. Our proposal of $H_2O_2$ formation in one-equiv. of $H^+$ induced $NO_2^-$ reduction was authenticated by comparing this spectrum with those of the authentic samples: (i) $H_2O_2$ plus **3** (8.66 ppm; ESI,† Fig. S15b) and (ii) $H_2O_2$ only (8.66 ppm; ESI,† Fig. S15c).[46] The amount of $H_2O_2$ in the above reaction was confirmed to be more than 50% (defining $\frac{1}{2}$ equivalent of $H_2O_2$ relative to **2** as 100% yield) from $^1$H-NMR spectral measurements and using benzene as the internal standard (ESI,† ES, and Fig. S15a).[46] Time-based $^1$H-NMR spectral measurements for the above reaction showed the gradual formation of $H_2O_2$ (8.66 ppm), which starts decreasing after reaching its maxima, suggesting the decomposition of $H_2O_2$ to $H_2O$ (Fig. 5a).[44,45] In addition to $^1$H-NMR, iodometric titration likewise confirmed $H_2O_2$ formation in the reaction of **2** with one-equiv. of $H^+$ which was determined to be ∼65% (ESI, ES, and Fig. S16a†) (defining 1/2 equivalent of $H_2O_2$ relative to **2** as 100% yield). However, no $H_2O_2$ was observed in iodometric titration when the reaction was carried out in the presence of two-equiv. of $H^+$ (ESI, ES, and Fig. S16b†).[47]

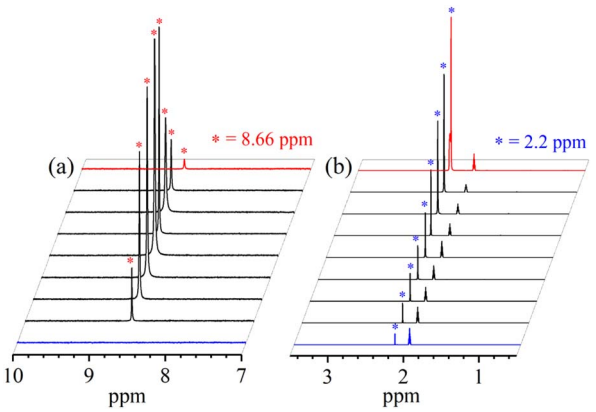


Fig. 5 1H-NMR spectrum of (a) $H_2O_2$ formation and (b) $H_2O$ formation in the reaction of **2** with one-equiv. & two-equiv. of $H^+$ in $CD_3CN$ recorded at different times, respectively.

Furthermore, we have also established $H_2O$ formation in the $NO_2^-$ reduction reaction in the presence of two-equiv. of $H^+$ by $^1$H-NMR spectroscopic measurements (Fig. 5b and S15d, ESI†). To establish that $H^+$ is only responsible for forming $^1$H-NMR signals at 2.2 ppm, we have explored the same reaction using $CF_3SO_3D$ ($D^+$ source). Surprisingly, when the source was $D^+$, we did not observe the formation of the $H_2O$ peak (at 2.2 ppm); this clearly suggests that $H^+$ ions are responsible for the $H_2O$ formation in the two-equiv. of $H^+$ induced $NO_2^-$ reduction (ESI, ES, and Fig. S17†). In addition, time-dependent $^1$H-NMR spectral measurements for the reaction of **2** with two-equiv. of $H^+$ showed an increment in the peak of $H_2O$ protons and a kind of first time-base measurement, further supporting our proposal of $H_2O$ formation (Fig. 5b). However, our efforts to quantify the amount of $H_2O$ formed in the reaction are futile; but they scientifically established the mechanistic aspect of acid-induced $NO_2^-$ reduction in the presence of different equivalents of $H^+$. These results are the only example where tracking $H^+$-induced $NO_2^-$ reduction products has confirmed that the variable amounts of $H^+$ (pH/acidic conditions) generate NO with $H_2O_2$ (one-equiv. of $H^+$) or $H_2O$ (≥two-equiv. of $H^+$).

Furthermore, we attempted to characterize the proposed $[Fe–ONOH]^{2+}$ intermediate to illustrate its conversion mechanism to **3**. However, after several attempts, we failed to detect/stabilize the intermediate even at low temperature (193 K) in UV-vis & FT-IR spectroscopic measurements, suggesting a kinetically driven reaction.[48] Since metal-nitrous acid intermediates are known to be highly unstable intermediates,[34b,36,40h–j] there are only a few reports about the metal-bound nitrous acid species.[34b,40h,40j,49] However, to support our mechanistic proposal for the formation of an $^{\bullet}OH$ radical ($H_2O_2$) *via* the homolytic cleavage of the N–O bond, we pursued the $^{\bullet}OH$ radical trapping experiment using 2,4-di-*tert*-butylphenol (2,4-DTBP).[50] In the one-equiv. of $H^+$ induced $NO_2^-$ reduction reaction, we have observed the formation of 3,5-Di-*tert*-butylcatechol (3,5-DTBC, ∼22%) and 2,4-DTBP-dimer (2,4-DTBP-D, ∼8%) with a minimal amount of nitro-2,4-DTBP ($NO_2$-2,4-DTBP, ∼6%) (ESI, ES, and Fig. S18 & S19†). The generation of 3,5-DTBC[51] in the above experiments undoubtedly confirmed the $^{\bullet}OH$ formation *via* the N–O bond homolysis of the ON–OH moiety. Hence, the formation of 3,5-DTBC and other products confirms the reaction sequences (Scheme 3) and supports the

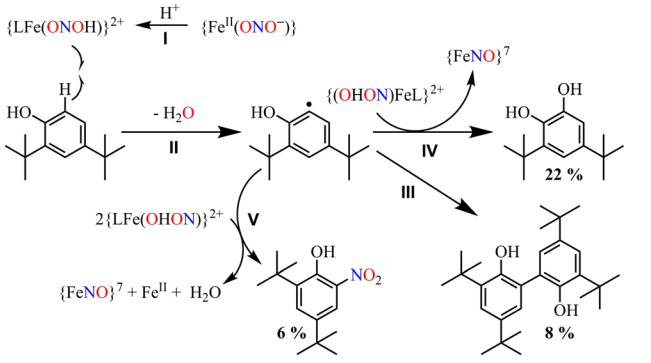


Scheme 3

Open Access Article. Published on 23 February 2023. Downloaded on 9/21/2023 12:58:10 AM. This article is licensed under a Creative Commons Attribution-NonCommercial 3.0 Unported Licence.

presence of the $[Fe\text{-}(ONOH)]^{2+}$ intermediate in the one-equiv. of $H^+$ induced $NO_2^-$ reduction reaction.

The transformation of 2,4-DTBP in the presence of one-equiv. of $H^+$ can be explained based on the radical coupling reaction.[51] The sequences of the 2,4-DTBP conversion are believed to be (i) the generation of the phenoxyl radical and the release of Fe–NOs by the H-atom abstraction reaction of $[Fe\text{–}ONOH]^{2+}$ from DTBP (Scheme 3, reaction I & II). After that, the phenoxyl radical either (ii) dimerizes to give 2,4-DTBP-D (Scheme 3, reaction III) or (iii) produces 3,5-DTBC upon radical coupling with another molecule of $[Fe\text{–}ONOH]^{2+}$ and releases **3** (Scheme 3, reaction IV). In some cases, $NO_2$-DTBP and **3** may generate in the presence of two molecules of $[Fe\text{–}ONOH]^{2+}$ and a phenoxyl radical (Scheme 3, reaction V). Also, when the above radical trapping experiments were performed using $CF_3SO_3D$, we observed the generation $^{\bullet}OD$-driven products of DTBC (ESI,† ES, and Fig. S20). In addition, we reacted **2**-$^{16}O^{14}N^{18}O^-$ with one equiv. of $H^+$ in the presence of 2,4-DTBP. Surprisingly, we observed the formation of 3,5-DTBC ($^{18}OH$) with $^{16}O^{14}N^{18}O$-DTBP as a side product (ESI, Fig. S21†). These experiments support that one equiv. of $H^+$ induced $NO_2^-$ reduction in **2** generates **3** + $H_2O_2$ *via* the homolytic cleavage of the N–O bond of the ON-OH intermediate.[36]

## Conclusion

The mechanistic investigation of acid-induced $NO_2^-$ reduction became an important research topic in modern-day chemistry as it deals with $NO_2^-$ to NO transformation, an essential signaling molecule in biosystems.[40b,52] The mechanistic aspects of NiR chemistry mediated by $H^+$ are still challenging to the scientific community and yet to be resolved as two different side products have been proposed to form *in vivo* and *in vitro* studies.[8a,9,16,25,30] Also, the pH/or $H^+$ ion concentration effect is yet to be confirmed as it affects the reaction mechanism and the side products of $NO_2^-$ reduction reactions.[48] In this report, we have shown the reduction of $NO_2^-$ in a nonheme $Fe^{II}$-nitrito complex, $[(12TMC)Fe^{II}(NO_2^-)]^+$ (**2**), to an Fe–nitrosyl complex $[(12TMC)Fe(NO)]^{2+}$, $\{FeNO\}^7$ (**3**), in the presence of different equivalents of $H^+$ ($CF_3SO_3D$, $D^+$ ion source), a biomimetic functional model of NiR. The structural details of $\{FeNO\}^7$ showed an axially coordinated NO moiety to the Fe center. In addition, $^{15}N$-labeled $^{15}NO_2^-$ experiments confirm that the N atom of the NO moiety in **3** is derived from the $NO_2^-$ anion of **2**. Acid-induced $NO_2^-$ reduction of **2** showed the formation of $\{FeNO\}^7$ along with $H_2O_2$ or $H_2O$ as a side product when treated with different ratios of $H^+$, one-equiv. or ≥two-equiv., respectively. Reports on acid-induced biomimetic $NO_2^-$ reduction[40h,j,43] and biological NiR reactions[9b,40g,41] suggested a metal-ONOH intermediate before NO formation; hence, we believe that the $H^+$-induced $NO_2^-$ reduction on the $Fe^{II}$ center in **2** should generate **3** *via* the proposed $[Fe\text{–}ONOH]^{2+}$ intermediate and follow the NiR chemistry. The N–O bond homolysis of the proposed ONOH intermediate was supported by the observation of 3,5-DTBC-$^{16}$ OH($^{18}$ OH) in $^{\bullet}OH$ radical trapping experiments using 2,4-DTBP[51] in the reaction of **2**-$ON^{16}O_2^-$($^{16}ON^{18}O^-$) with one equiv. of $H^+$. Also, the observation of DTBC(OD) in the presence of $D^+$ further supports the acid-induced reduction of $NO_2^-$. In addition, a significant amount of $H_2O_2$ formation was also confirmed using $^1$H-NMR/or UV-vis iodometric titration along **3**.[46] However, the generation of the $H_2O$ molecule was believed to occur either (i) by $NO_2^-$ reduction in the presence of two-equiv. of $H^+$ and an electron[9b,40c,40g,40h,40j] or (ii) by the acid-induced decay of $H_2O_2$ or auto-decomposition of $H_2O_2$.[44,45] The redox potential of **2** was higher than that of the enzymatic iron-site, making **2** more prone to reduction.[53] At this time, we are not sure about the source of another electron; however, we are currently exploring various $NO_2^-$ bound $Cu^{I/II}$ & $Fe^{II/III}$ complexes to understand the reaction sequences and track the electron source using the known electron donor species. These results provide entirely new reaction sequences for acid-induced $NO_2^-$ reduction chemistry, a functional model of biomimetic NiR chemistry, and show how the $H^+$ ion concentration determines $H_2O_2$ or $H_2O$ as a side product along with NO.

## Experimental Section

For the experimental details, see the ESI.†

## Data availability

All the required data is already provided in the ESI† and manuscript.

## Author contributions

PKK discovered /conceptualized the initial project. Kulbir carried out most of the experiments and gathered the data. PKK, SG & TD helped in interpreting the experimental results. SCS, Kulbir & SD worked on growing the crystals and recording the crystallographic data. Kulbir and SD write the first draft of the article. PKK & TD have corrected the manuscript, finalized the final draft, and guided during the revision. PKK followed and guided the whole project work.

## Conflicts of interest

There are no conflicts to declare.

## Acknowledgements

This work was supported by a grants-in-aid (Grant No. CRG/2021/003371, & EEQ/2021/000109) from SERB-DST and AvH (ID: 1219648). Kulbir and S. D. thank IISER Tirupati for their fellowship.

## References

1 (*a*) R. F. Furchgott, *Angew. Chem., Int. Ed.*, 1999, **38**, 1870–1880; (*b*) L. J. Ignarro, *Angew. Chem., Int. Ed.*, 1999, **38**, 1882–1892; (*c*) L. J. Ignarro, *Nitric Oxide: Biology and Pathobiology*, Academic press, 2000; (*d*) G. B. Richter-Addo, P. Legzdins and J. Burstyn, *Chem. Rev.*, 2002, **102**, 857–860;


© 2023 The Author(s). Published by the Royal Society of Chemistry

Open Access Article. Published on 23 February 2023. Downloaded on 9/21/2023 12:58:10 AM. This article is licensed under a Creative Commons Attribution-NonCommercial 3.0 Unported Licence.

(*e*) I. M. Wasser, S. de Vries, P. Moënne-Loccoz, I. Schröder and K. D. Karlin, *Chem. Rev.*, 2002, **102**, 1201–1234.

2 R. B. S. Nabi, R. Tayade, A. Hussain, K. P. Kulkarni, Q. M. Imran, B. G. Mun and B. W. Yun, *Environ. Exp. Bot.*, 2019, **161**, 120–133.

3 F. Vargas, J. M. Moreno, R. Wangensteen, I. Rodriguez-Gomez and J. Garcia-Estan, *Eur. J. Endocrinol.*, 2007, **156**, 1–12.

4 (*a*) H. T. Dong, S. Camarena, D. Sil, M. O. Lengel, J. Zhao, M. Y. Hu, E. E. Alp, C. Krebs and N. Lehnert, *J. Am. Chem. Soc.*, 2022, **144**, 16395–16409; (*b*) D. J. Stuehr, S. S. Gross, I. Sakuma, R. Levi and C. F. Nathan, *J. Exp. Med.*, 1989, **169**, 1011–1020.

5 (*a*) R. E. Huie and S. Padmaja, *Free Radical Res. Commun.*, 1993, **18**, 195–199; (*b*) P. Pacher, J. S. Beckman and L. Liaudet, *Physiol. Rev.*, 2007, **87**, 315–424; (*c*) C. Prolo, M. N. Alvarez and R. Radi, *Biofactors*, 2014, **40**, 215–225.

6 (*a*) W. C. Nottingham and J. R. Sutter, *Int. J. Chem. Kinet.*, 1986, **18**, 1289–1302; (*b*) C. H. Lim, P. C. Dedon and W. M. Deen, *Chem. Res. Toxicol.*, 2008, **21**, 2134–2147.

7 (*a*) R. Radi, *Proc. Natl. Acad. Sci. U. S. A.*, 2004, **101**, 4003–4008; (*b*) B. Kalyanaraman, *Proc. Natl. Acad. Sci. U. S. A.*, 2004, **101**, 11527–11528; (*c*) P. C. Dedon and S. R. Tannenbaum, *Arch. Biochem. Biophys.*, 2004, **423**, 12–22.

8 (*a*) N. Lehnert, T. C. Berto, M. G. I. Galinato and L. E. Goodrich, in *Handbook of Porphyrin Science*, ed. K. Kadish, K. Smith and R. Guilard, World Scientific Publishing, Singapore, 2011, p. 1; (*b*) T. B. McCall, N. K. Boughton-Smith, R. M. Palmer, B. J. Whittle and S. Moncada, *Biochem. J.*, 1989, **261**, 293–296; (*c*) R. G. Knowles and S. Moncada, *Biochem. J.*, 1994, **298**(Pt 2), 249–258.

9 (*a*) B. A. Averill, *Chem. Rev.*, 1996, **96**, 2951–2964; (*b*) E. I. Tocheva, F. I. Rosell, A. G. Mauk and M. E. Murphy, *Science*, 2004, **304**, 867–870.

10 L. Ma, L. Hu, X. Feng and S. Wang, *Aging Dis.*, 2018, **9**, 938–945.

11 (*a*) P. C. Ford and I. M. Lorkovic, *Chem. Rev.*, 2002, **102**, 993–1018; (*b*) M. P. Schopfer, B. Mondal, D. H. Lee, A. A. Sarjeant and K. D. Karlin, *J. Am. Chem. Soc.*, 2009, **131**, 11304–11305; (*c*) M. P. Doyle and J. W. Hoekstra, *J. Inorg. Biochem.*, 1981, **14**, 351–358; (*d*) M. Yenuganti, S. Das, K. Kulbir, S. Ghosh, P. Bhardwaj, S. S. Pawar, S. C. Sahoo and P. Kumar, *Inorg. Chem. Front.*, 2020, **7**, 4872–4882.

12 (*a*) E. Weitzberg and J. O. Lundberg, *Nitric Oxide – Biol. Chem.*, 1998, **2**, 1–7; (*b*) J. O. Lundberg and M. Govoni, *Free Radical Biol. Med.*, 2004, **37**, 395–400.

13 (*a*) L. I. Hochstein and G. A. Tomlinson, *Annu. Rev. Microbiol.*, 1988, **42**, 231–261; (*b*) W. H. Campbell, *Annu. Rev. Plant Physiol. Plant Mol. Biol.*, 1999, **50**, 277–303.

14 P. Tavares, A. S. Pereira, J. J. Moura and I. Moura, *J. Inorg. Biochem.*, 2006, **100**, 2087–2100.

15 N. Lehnert, E. Kim, H. T. Dong, J. B. Harland, A. P. Hunt, E. C. Manickas, K. M. Oakley, J. Pham, G. C. Reed and V. S. Alfaro, *Chem. Rev.*, 2021, **121**, 14682–14905.

16 N. Benjamin, F. O'Driscoll, H. Dougall, C. Duncan, L. Smith, M. Golden and H. McKenzie, *Nature*, 1994, **368**, 502.

17 J. O. Lundberg, E. Weitzberg, J. M. Lundberg and K. Alving, *Gut*, 1994, **35**, 1543–1546.

18 (*a*) S. Kundu, W. Y. Kim, J. A. Bertke and T. H. Warren, *J. Am. Chem. Soc.*, 2017, **139**, 1045–1048; (*b*) K. Cosby, K. S. Partovi, J. H. Crawford, R. P. Patel, C. D. Reiter, S. Martyr, B. K. Yang, M. A. Waclawiw, G. Zalos, X. Xu, K. T. Huang, H. Shields, D. B. Kim-Shapiro, A. N. Schechter, R. O. Cannon and M. T. Gladwin, *Nat. Med.*, 2003, **9**, 1498–1505; (*c*) U. B. Hendgen-Cotta, M. W. Merx, S. Shiva, J. Schmitz, S. Becher, J. P. Klare, H.-J. Steinhoff, A. Goedecke, J. Schrader, M. T. Gladwin, M. Kelm and T. Rassaf, *Proc. Natl. Acad. Sci. U. S. A.*, 2008, **105**, 10256–10261.

19 J. Brooks and D. Keilin, *Proc. R. Soc. London, Ser. B*, 1937, **123**, 368–382.

20 M. Kumar, N. A. Dixon, A. C. Merkle, M. Zeller, N. Lehnert and E. T. Papish, *Inorg. Chem.*, 2012, **51**, 7004–7006.

21 (*a*) S. Hematian, M. A. Siegler and K. D. Karlin, *J. Am. Chem. Soc.*, 2012, **134**, 18912–18915; (*b*) S. Hematian, I. Kenkel, T. E. Shubina, M. Dürr, J. J. Liu, M. A. Siegler, I. Ivanovic-Burmazovic and K. D. Karlin, *J. Am. Chem. Soc.*, 2015, **137**, 6602–6615.

22 M. E. Murphy, S. Turley and E. T. Adman, *J. Biol. Chem.*, 1997, **272**, 28455–28460.

23 R. C. Maji, S. K. Barman, S. Roy, S. K. Chatterjee, F. L. Bowles, M. M. Olmstead and A. K. Patra, *Inorg. Chem.*, 2013, **52**, 11084–11095.

24 A. P. Hunt, A. E. Batka, M. Hosseinzadeh, J. D. Gregory, H. K. Haque, H. Ren, M. E. Meyerhoff and N. Lehnert, *ACS Catal.*, 2019, **9**, 7746–7758.

25 T. S. Kurtikyan, A. A. Hovhannisyan, A. V. Iretskii and P. C. Ford, *Inorg. Chem.*, 2009, **48**, 11236–11241.

26 (*a*) B. C. Sanders, S. M. Hassan and T. C. Harrop, *J. Am. Chem. Soc.*, 2014, **136**, 10230–10233; (*b*) S. Zhang, M. M. Melzer, S. N. Sen, N. Celebi-Olcum and T. H. Warren, *Nat. Chem.*, 2016, **8**, 663–669.

27 (*a*) L. Cheng, D. R. Powell, M. A. Khan and G. B. Richter-Addo, *Chem. Commun.*, 2000, 2301–2302, DOI: **10.1039/B006775J**; (*b*) A. K. Patra, R. K. Afshar, J. M. Rowland, M. M. Olmstead and P. K. Mascharak, *Angew. Chem., Int. Ed. Engl.*, 2003, **42**, 4517–4521.

28 K. Kulbir, S. Das, T. Devi, M. Goswami, M. Yenuganti, P. Bhardwaj, S. Ghosh, S. C. Sahoo and P. Kumar, *Chem. Sci.*, 2021, **12**, 10605–10612.

29 S. Hong, J. J. Yan, D. G. Karmalkar, K. D. Sutherlin, J. Kim, Y. M. Lee, Y. Goo, P. K. Mascharak, B. Hedman, K. O. Hodgson, K. D. Karlin, E. I. Solomon and W. Nam, *Chem. Sci.*, 2018, **9**, 6952–6960.

30 (*a*) J. Heinecke and P. C. Ford, *Coord. Chem. Rev.*, 2010, **254**, 235–247; (*b*) S. Das, K. Kulbir, S. Ghosh, S. Chandra Sahoo and P. Kumar, *Chem. Sci.*, 2020, **11**, 5037–5042; (*c*) S. Das, K. Kulbir, S. Ray, T. Devi, S. Ghosh, S. S. Harmalkar, S. N. Dhuri, P. Mondal and P. Kumar, *Chem. Sci.*, 2022, **13**, 1706–1714.

31 (*a*) A. P. Hunt and N. Lehnert, *Acc. Chem. Res.*, 2015, **48**, 2117–2125; (*b*) A. L. Speelman, B. Zhang, C. Krebs and N. Lehnert, *Angew. Chem., Int. Ed.*, 2016, **55**, 6685–6688.

© 2023 The Author(s). Published by the Royal Society of Chemistry

Open Access Article. Published on 23 February 2023. Downloaded on 9/21/2023 12:58:10 AM. This article is licensed under a Creative Commons Attribution-NonCommercial 3.0 Unported Licence.

32 (*a*) P. Kumar, Y. M. Lee, Y. J. Park, M. A. Siegler, K. D. Karlin and W. Nam, *J. Am. Chem. Soc.*, 2015, **137**, 4284–4287; (*b*) P. Kumar, Y. M. Lee, L. Hu, J. Chen, Y. J. Park, J. Yao, H. Chen, K. D. Karlin and W. Nam, *J. Am. Chem. Soc.*, 2016, **138**, 7753–7762; (*c*) S. Hong, J. J. Yan, D. G. Karmalkar, K. D. Sutherlin, J. Kim, Y. M. Lee, Y. Goo, P. K. Mascharak, B. Hedman, K. O. Hodgson, K. D. Karlin, E. I. Solomon and W. Nam, *Chem. Sci.*, 2018, **9**, 6952–6960.

33 (*a*) J. L. Heinecke, C. Khin, J. C. Pereira, S. A. Suarez, A. V. Iretskii, F. Doctorovich and P. C. Ford, *J. Am. Chem. Soc.*, 2013, **135**, 4007–4017; (*b*) T. S. Kurtikyan, A. A. Hovhannisyan and P. C. Ford, *Inorg. Chem.*, 2016, **55**, 9517–9520.

34 (*a*) B. A. Averill, *Chem. Rev.*, 1996, **96**, 2951–2964; (*b*) M. A. Puthiyaveetil Yoosaf, S. Ghosh, Y. Narayan, M. Yadav, S. C. Sahoo and P. Kumar, *Dalton Trans.*, 2019, **48**, 13916–13920.

35 C. Uyeda and J. C. Peters, *J. Am. Chem. Soc.*, 2013, **135**, 12023–12031.

36 W. M. Ching, P. P. Chen and C. H. Hung, *Dalton Trans.*, 2017, **46**, 15087–15094.

37 C. H. Hsieh, S. Ding, O. F. Erdem, D. J. Crouthers, T. Liu, C. C. McCrory, W. Lubitz, C. V. Popescu, J. H. Reibenspies, M. B. Hall and M. Y. Darensbourg, *Nat. Commun.*, 2014, **5**, 3684.

38 (*a*) S. Goswami, D. Sen, N. K. Das, H. K. Fun and C. K. Quah, *Chem. Commun.*, 2011, **47**, 9101–9103; (*b*) J. Chen, H. Yoon, Y. M. Lee, M. S. Seo, R. Sarangi, S. Fukuzumi and W. Nam, *Chem. Sci.*, 2015, **6**, 3624–3632; (*c*) Y. M. Lee, M. Yoo, H. Yoon, X. X. Li, W. Nam and S. Fukuzumi, *Chem. Commun.*, 2017, **53**, 9352–9355.

39 (*a*) P. C. Ford, J. C. M. Pereira and K. M. Miranda, in *Nitrosyl Complexes in Inorganic Chemistry, Biochemistry and Medicine II*, ed. D. M. P. Mingos, Springer Berlin Heidelberg, Berlin, Heidelberg, 2014, pp. 12–44, DOI: DOI: 10.1007/430_2013_117; (*b*) G. R. Wyllie and W. R. Scheidt, *Chem. Rev.*, 2002, **102**, 1067–1090; (*c*) D. M. P. Mingos, in *Nitrosyl Complexes in Inorganic Chemistry, Biochemistry and Medicine I*, ed. D. M. P. Mingos, Springer Berlin Heidelberg, Berlin, Heidelberg, 2014, pp. 1–44, DOI: DOI: 10.1007/430_2013_116.

40 (*a*) Y. Li, M. Hodak and J. Bernholc, *Biochemistry*, 2015, **54**, 1233–1242; (*b*) O. Einsle, A. Messerschmidt, R. Huber, P. M. Kroneck and F. Neese, *J. Am. Chem. Soc.*, 2002, **124**, 11737–11745; (*c*) S. Basu, N. A. Azarova, M. D. Font, S. B. King, N. Hogg, M. T. Gladwin, S. Shiva and D. B. Kim-Shapiro, *J. Biol. Chem.*, 2008, **283**, 32590–32597; (*d*) S. Besson, C. Carneiro, J. J. Moura, I. Moura and G. Fauque, *Anaerobe*, 1995, **1**, 219–226; (*e*) M. J. Boulanger, M. Kukimoto, M. Nishiyama, S. Horinouchi and M. E. Murphy, *J. Biol. Chem.*, 2000, **275**, 23957–23964; (*f*) J. Brooks and D. Keilin, *Proc. R. Soc. London, Ser. B*, 1937, **123**, 368–382; (*g*) S. L. Rose, S. V. Antonyuk, D. Sasaki, K. Yamashita, K. Hirata, G. Ueno, H. Ago, R. R. Eady, T. Tosha, M. Yamamoto and S. S. Hasnain, *Sci. Adv.*, 2021, **7**, eabd8523; (*h*) M. Kujime and H. Fujii, *Angew. Chem., Int. Ed. Engl.*, 2006, **45**, 1089–1092; (*i*) S. Maekawa, T. Matsui, K. Hirao and Y. Shigeta, *J. Phys. Chem. B*, 2015, **119**, 5392–5403; (*j*) S. C. Hsu, Y. L. Chang, W. J. Chuang, H. Y. Chen, I. J. Lin, M. Y. Chiang, C. L. Kao and H. Y. Chen, *Inorg. Chem.*, 2012, **51**, 9297–9308.

41 M. Lintuluoto and J. M. Lintuluoto, *Metallomics*, 2018, **10**, 565–578.

42 (*a*) B. Chen, Y. Xia, R. He, H. Sang, W. Zhang, J. Li, L. Chen, P. Wang, S. Guo, Y. Yin, L. Hu, M. Song, Y. Liang, Y. Wang, G. Jiang and R. N. Zare, *Proc. Natl. Acad. Sci. U. S. A.*, 2022, **119**, e2209056119; (*b*) P. Ulanski and C. von Sonntag, *J. Chem. Soc., Perkin Trans. 2*, 1999, 165–168, DOI: 10.1039/a808543i.

43 J. A. Halfen, S. Mahapatra, E. C. Wilkinson, A. J. Gengenbach, V. G. Young, L. Que and W. B. Tolman, *J. Am. Chem. Soc.*, 1996, **118**, 763–776.

44 (*a*) B. Mlasi, D. Glasser and D. Hildebrandt, *Ind. Eng. Chem. Res.*, 2015, **54**, 5589–5597; (*b*) F. M. Fomin and K. S. Zaitseva, *Russ. J. Phys. Chem. A*, 2014, **88**, 466–470.

45 P. Pędziwiatr, F. Mikołajczyk, D. Zawadzki, K. Mikołajczyk and A. Bedka, *Acta Innov.*, 2018, 45–52, DOI: 10.32933/ActaInnovations.26.5.

46 N. A. Stephenson and A. T. Bell, *Anal. Bioanal. Chem.*, 2005, **381**, 1289–1293.

47 K. Mase, K. Ohkubo, Z. Xue, H. Yamada and S. Fukuzumi, *Chem. Sci.*, 2015, **6**, 6496–6504.

48 (*a*) Z. H. L. Abraham, B. E. Smith, B. D. Howes, D. J. Lowe and R. R. Eady, *Biochem. J.*, 1997, **324**, 511–516; (*b*) Z. Huang, S. Shiva, D. B. Kim-Shapiro, R. P. Patel, L. A. Ringwood, C. E. Irby, K. T. Huang, C. Ho, N. Hogg, A. N. Schechter and M. T. Gladwin, *J. Clin. Invest.*, 2005, **115**, 2099–2107; (*c*) C. A. Clark, C. P. Reddy, H. Xu, K. N. Heck, G. H. Luo, T. P. Senftle and M. S. Wong, *ACS Catal.*, 2020, **10**, 494–509; (*d*) H.-Y. Hu, N. Goto and K. Fujie, *Water Res.*, 2001, **35**, 2789–2793.

49 (*a*) A. Samouilov, P. Kuppusamy and J. L. Zweier, *Arch. Biochem. Biophys.*, 1998, **357**, 1–7; (*b*) K. Tsuchiya, Y. Kanematsu, M. Yoshizumi, H. Ohnishi, K. Kirima, Y. Izawa, M. Shikishima, T. Ishida, S. Kondo, S. Kagami, Y. Takiguchi and T. Tamaki, *Am. J. Physiol. Heart Circ.*, 2005, **288**, H2163–H2170.

50 A. Dubey, V. Rives and S. Kannan, *J. Mol. Catal. A: Chem.*, 2002, **181**, 151–160.

51 (*a*) A. Arnold, R. Metzinger and C. Limberg, *Chemistry*, 2015, **21**, 1198–1207; (*b*) C. Citek, C. T. Lyons, E. C. Wasinger and T. D. Stack, *Nat. Chem.*, 2012, **4**, 317–322; (*c*) P. T. Kaye, K. W. Wellington and G. M. Watkins, *Arkivoc*, 2010, **2009**, 301–313.

52 S. Suzuki, K. Kataoka and K. Yamaguchi, *Acc. Chem. Res.*, 2000, **33**, 728–735.

53 C. E. Immoos, J. Chou, M. Bayachou, E. Blair, J. Greaves and P. J. Farmer, *J. Am. Chem. Soc.*, 2004, **126**, 4934–4942.


© 2023 The Author(s). Published by the Royal Society of Chemistry